

Epidemiological Parameters of SARS-CoV-2 in the UK during the 2023/2024 Winter: A Cohort Study

Christopher E. Overton^{*1,2}, Martyn Fyles², Jonathon Mellor², Robert S. Paton², Alexander M. Phillips^{2,3}, Alex Glaser², Andre Charlett⁴, and Thomas Ward²

¹ *Department for Mathematical Sciences, University of Liverpool*

² *Infectious Disease Modelling Team, All Hazards Intelligence, Data Analytics and Surveillance, UK Health Security Agency*

³ *Department for Electrical Engineering and Electronics, University of Liverpool*

⁴ *Statistics, Modelling, and Economics, Analytics & Data Science, Data Analytics and Surveillance, UK Health Security Agency*

*Corresponding author: c.overton@liverpool.ac.uk

Abstract

Estimating epidemiological parameters is essential for informing an effective public health response during waves of infectious disease transmission. However, many parameters are challenging to estimate from real-world data, and rely on human challenge studies or mass community testing. During Winter 2023/2024, a community cohort study of SARS-CoV-2 was conducted across households in England and Scotland. From this survey, questionnaire data and follow-up testing protocols provided valuable data into multiple epidemiological parameters: namely, the duration of positivity, test sensitivity, and the incubation period. Here, Bayesian statistical modelling methods are developed and applied to estimate the underlying parameters. The duration of LFD positivity is found to increase with increasing age, with a mean of 8.55 days (95% CrI: 7.65 days, 9.44 days) in the youngest age group compared to 10.27 days (95% CrI: 9.85 days, 10.71 days) in the oldest age group. Similarly, test sensitivity, as a function of time since symptom onset, decays fastest in the youngest age group, reaching a minimum sensitivity of 0.26 (95% CrI: 0.16, 0.37) compared to 0.54 (95% CrI: 0.46, 0.6). Such patterns are expected since younger individuals experience less severe symptoms of COVID-19 and are likely to clear the virus faster. Combining the duration of positivity and test sensitivity, we estimate the probability of returning a positive test. Close to symptom onset date, this probability is approximately 95%. However, this rapidly drops off, dropping below 5% after 11.3 days (95% CrI: 9.7 days, 13 days) for the youngest age group and 16.2 days (95% CrI: 15.4 days, 17.1 days) for the oldest age group. For the incubation period, there is no clear pattern by age. Across all age groups, the mean incubation period is 2.52 days (95% CrI: 2.42 days, 2.62 days). This is shorter than the most recent estimates for Omicron BA.5, which is in line with earlier research that found replacing variants had shorter incubation periods.

Key words

COVID-19; sensitivity; incubation period; positivity; duration

1. Introduction

SARS-CoV-2, the virus that causes COVID-19, continues to cause resurgent global epidemics. The emergence of novel variants of SARS-CoV-2 has been driven by mutation from selective pressures and within-host factors. These mutations can lead to viral phenotypic changes that impact epidemiological parameters, such as the lower risk of mortality with Omicron relative to Delta [1–5], or shorter incubation periods of replacing variants [6–8]. To inform an effective public health response, understanding how these parameters change is vital for surveillance and policy.

8 During the height of the pandemic, mass testing data [9] and contact tracing data [10], alongside
9 controlled studies, such as human challenge studies [11], were a valuable source of data on many
10 epidemiological parameters, such as the incubation period and duration of positivity. Since April
11 2022, these surveillance efforts have been scaled down in the UK, with the Office for National
12 Statistics (ONS) COVID-19 Infection Survey (CIS) concluding in March 2023. Similar reductions in
13 surveillance data occurred globally, leading to uncertainty in these parameters. During Winter 23/24,
14 the UK Health Security Agency (UKHSA) and ONS conducted a new community prevalence study to
15 determine SARS-CoV-2 dynamics in England and Scotland. In this study, a randomly sampled cohort
16 were tested using Lateral Flow Device (LFD) tests independently of symptom status to evaluate the
17 trends of SARS-CoV-2 in the community [12]. However, as part of the study design, additional data
18 were collected that provides valuable insights into multiple epidemiological parameters.

19 In this paper, data from this survey are used to estimate the duration of LFD positivity, LFD test
20 sensitivity, and the current incubation period (the time from becoming infected to developing
21 symptoms) of SARS-CoV-2. The most recent estimates of these parameters are limited to the pre-
22 Alpha [13], Omicron BA.1 and BA.2 [14], and Omicron BA.5 [8,15] periods, respectively, reducing
23 their utility in current public health policy. These parameters are essential in modelling/designing
24 different interventions or public health messaging, as well as important parts of infectious disease
25 surveillance tools. By providing estimates for these parameters during Winter 23/24, we gain insight
26 into the current state of the virus.

27 **2. Data**

28 The UKHSA Winter Coronavirus Infection Survey (WCIS) builds on the success of the ONS CIS survey,
29 and uses a subset of the same sample population. Around 150,000 individuals were invited to take
30 part in the study, which ran from 13/11/2023 to 27/03/2024. The study design is described in the
31 Supplementary Material.

32 Upon recruitment to the study, participants were provided with 14 SARS-CoV-2 LFD tests and were
33 asked to complete a test every four weeks. Participants then had a 10-day window within which to
34 complete those tests. Upon a participant testing positive, they were asked to complete a short
35 questionnaire and to complete a follow-up testing protocol by continuing to test every other day
36 until two consecutive negative results are observed. This repeat testing protocol, a modification
37 from the design of the original ONS CIS, provides key data for estimating sensitivity and the duration
38 of positivity.

39 A study participant is defined as an individual who returned at least one test result. There were
40 123,243 participants, of which 6,395 returned at least one positive test result. A total of 426,667
41 tests were performed as part of the main survey, of which 6,466 were positive. This averages 3.46
42 tests returned per participant that returned at least one test. This analysis is restricted to
43 participants who returned at least one positive test result.

44 Unlike the original ONS CIS, participants were not compensated for their participation in the study.
45 In addition, because of the re-use of the previous ONS CIS cohort, older individuals were over-
46 represented in the sample. A demographic breakdown of the overall study participants is provided in
47 the Supplementary Table 1. An age breakdown of study participants used in each model is provided
48 in Table 1. Data inclusion criteria for each model are described in the corresponding methods
49 sections.

50

Table 1: Age breakdown of the participants included in each model.

Age group	Duration of Positivity (N=4,567)	Sensitivity (N=3,584)	Incubation period (N=1405)
3 to 17 years	102 (2.2%)	122 (3.4%)	3 (0.2%)
18 to 34 years	158 (3.5%)	78 (2.2%)	59 (4.2%)
35 to 44 years	451 (9.9%)	360 (10.0%)	95 (6.8%)
45 to 54 years	801 (17.5%)	630 (17.6%)	155 (11.0%)
55 to 64 years	1,313 (28.7%)	1,027 (28.7%)	414 (29.5%)
65 to 74 years	1,193 (26.1%)	933 (26.0%)	481 (34.2%)
75 years and over	549 (12.0%)	434 (12.1%)	198 (14.1%)

51 3. Methods

52 All methods used in this paper are Bayesian methods, implemented in the Stan [16] programming
53 language, using CmdStanR [17] interfaced through R [18]. For each model, 4 chains were run
54 generating 1000 samples each, with a warmup period of 1000 samples. Convergence of the models
55 was assessed using the \hat{R} statistic [19], with a convergence threshold of $\hat{R} < 1.01$.

56 3.1. Duration of LFD positivity

57 Understanding the duration an individual tests positive for is essential to understand the progression
58 of a disease. For example, if isolation policies are based on individuals testing positive, it is important
59 to know the duration of positivity, to determine whether this overlaps with the duration of
60 infectiousness [20]. The duration of positivity is also vital to understand when calculating the
61 incidence rate of new infections from a prevalence estimate.

62 The follow-up testing protocol provides interval-censored data on when individuals are no longer
63 testing positive. Determining when an individual would start testing positive is challenging, since it
64 will be left-censored at the date when they return their first positive test. To handle this, we instead
65 calculate the duration of LFD positivity as a function of time since symptom onset date, which is
66 reported in our data for 79% of individuals with at least one positive test. The symptom onset date is
67 interval censored on the date that participants reported developing symptoms. We note, however,
68 that only 8 positive tests occurred prior to the self-reported symptom onset of a case. This is
69 expected since antigen levels only start to rise very close to symptom onset date [21].

70 For inclusion in the duration of positivity model data, data on an individual's first positive test were
71 linked to data from their follow-up testing. From this, the dates of the first positive test and last
72 positive test were calculated. Data were cleaned by removing individuals with inconsistent testing
73 dates. Of the 6395 individuals who submitted a positive test in the main survey, 4599 had a
74 corresponding record in the repeat testing data. 32 records were removed due to inconsistent
75 testing dates, leaving a final sample size of 4567 individuals. For the 8 individuals with positive tests
76 prior to symptom onset date, we treat these as asymptomatic infections.

77 We consider two random variables, the time of symptom onset, S , and the time of last positive, L ,
78 where $L > S$. We are interested in the distribution of times between these two events, which we
79 denote by the random variable $\tau \in \mathbb{R}_+$. Both types of data are considered interval censored:

- 80 • $S \in [s_1, s_2]$, where $s_1 =$ "Symptom onset date" and $s_2 =$
81 "Symptom onset date plus 24 hours"
- 82 • $L \in [l_1, l_2]$, where $l_1 =$ "Last positive test date" and $l_2 =$
83 "First negative test date plus 24 hours".

84 The 24 hours are added to each event since we only know the date and not the time of each event,
 85 so it could happen any time within that 24-hour window. Note that for l_2 , we only consider negative
 86 tests that occur after the last positive date, assuming that any earlier negatives are false negatives.

87 If the individual did not return any negative tests during their follow up testing, then $l_2 = \infty$, i.e., the
 88 data are right-censored. If the individual does not have a symptom onset date, we treat the data as
 89 left-censored by the date of the first positive test, i.e., $s_1 = -\infty$ and $s_2 =$
 90 "First positive test date plus 24 hours". Based on these different censoring scenarios, there are
 91 four possible combinations that a data point can experience: (i) double-interval censoring, where the
 92 end points of each censoring interval are known; (ii) right-censoring, where the first event is interval
 93 censored and the second event is right-censored; (iii) left-censoring, where the first event is left-
 94 censored and the second event is interval censored; and (iv) left and right censoring, where the first
 95 event is left-censored and the second event is right censored. In each of these scenarios, we have a
 96 slightly different likelihood function. By considering distinct likelihood functions we make the model
 97 computationally feasible.

98 (i) *Doubly-interval censored data*

99 To model the duration of positivity, we wish to evaluate the following likelihood function

$$\begin{aligned}
 100 \quad \mathbb{P}(l_1 < L < l_2 \cap s_1 < S < s_2) &= \int_{s_1}^{s_2} \int_{l_1}^{l_2} f_{L,S}(L = l, S = s) dl ds \\
 101 &= \int_{s_1}^{s_2} \int_{l_1}^{l_2} f_{L,S}(L = l^* | S = s^*) f_S(S = s) dl ds \\
 102 &= \int_{s_1}^{s_2} \int_{l_1}^{l_2} f_P(l - s) f_S(S = s) dl ds, \tag{1}
 \end{aligned}$$

103 where f_P is the probability density function of the duration of positivity distribution. Implementing
 104 the likelihood in this form requires numerically evaluating a double integral, which is
 105 computationally expensive. Instead, we opt to use a latent variable approach [22–24], where we
 106 assume uniform prior distributions across the interval censored windows, i.e., $f_L(L = l) = \frac{1}{l_2 - l_1}$ and
 107 $f_S(S = s) = \frac{1}{s_2 - s_1}$, and sample the values of S and L from within their intervals by implementing:

$$108 \quad l^* \sim \text{Uniform}(l_1, l_2),$$

$$109 \quad s^* \sim \text{Uniform}(s_1, s_2),$$

$$110 \quad \text{Likelihood} = f_P(l^* - s^*).$$

111 Here, since l^* follows a uniform distribution, adding the probability density function of l^* to the
 112 integrand in Equation (1) (which is implicitly done by the latent variable method) will not affect the
 113 results since it only adds a constant to the integrand.

114 (ii) *Right-censored data*

115 If our data are right-censored, the likelihood function is

$$\begin{aligned}
 116 \quad \mathbb{P}(l_1 < L < \infty \cap s_1 < S < s_2) &= \int_{s_1}^{s_2} \int_{l_1}^{\infty} f_P(l - s) f_S(S = s) dl ds \\
 117 &= \int_{s_1}^{s_2} f_S(S = s) (1 - F_P(l_1 - s)) ds.
 \end{aligned}$$

118 We again use a latent variable approach, but only a single latent variable is needed:

$$119 \quad s^* \sim \text{Uniform}(s_1, s_2),$$

$$120 \quad \text{Likelihood} = 1 - F_P(l_1 - s^*).$$

121 (iii) *Left-censored data*

122 Following similar logic to the right-censored model, if our data are left-censored, the likelihood
123 function is

$$124 \quad \mathbb{P}(l_1 < L < l_2 \cap -\infty < S < s_2) = \int_{-\infty}^{s_2} \int_{l_1}^{l_2} f_P(l - s) f_S(S = s) dl ds \propto \int_{l_1}^{l_2} 1 - F_P(l - s_2) dl,$$

125 where an improper flat prior is implicitly used to model $f_S(S = s) = c \forall s \in [-\infty, s_2]$. Using latent
126 variables, we model this as

$$127 \quad l^* \sim \text{Uniform}(l_1, l_2),$$

$$128 \quad \text{Likelihood} = 1 - F_P(l^* - s_2).$$

129 (iv) *Left and right censored data*

130 If the data are both left and right censored, we have

$$131 \quad \mathbb{P}(l_1 < L < \infty \cap -\infty < S < s_2) = \int_{-\infty}^{s_2} \int_{l_1}^{\infty} f_P(l - s) f_S(S = s) dl ds \propto \int_{l_1}^{\infty} 1 - F_P(l - s_2) dl,$$

132 where an improper flat prior is implicitly used to model $f_S(S = s) = c \forall s \in [-\infty, s_2]$. To solve this
133 exactly would require numerically evaluating the integral or a latent variable approach with a
134 uniform latent variable bounded between l_1 to ∞ . To avoid any issues with using such an improper
135 prior, we can instead rewrite the model in terms of a single random variable

$$136 \quad \int_{-\infty}^{s_2} \int_{l_1}^{\infty} f_P(l - s) dl ds = \int_{l_1 - s_2}^{\infty} g(t) f_P(t) dt,$$

137 where $g(l - s)$ is the probability density function of the random variable $L - S$. We can
138 approximate this by assuming $g(\cdot)$ follows a uniform distribution, which gives

$$139 \quad \mathbb{P}(l_1 < L < \infty \cap -\infty < S < s_2) \approx \int_{l_1 - s_2}^{\infty} f_P(t) dt.$$

140 Therefore, the likelihood is given by

$$141 \quad \text{Likelihood} = 1 - F_P(l_1 - s_2).$$

142 Under the assumptions of uniform prior distributions for $f_L(L = l)$ and $f_S(S = s)$, the random
143 variable $L - S$ follows a trapezoidal distribution [22,23]. Here, we approximate a trapezoidal
144 distribution spanning from $(l_1 - s_2, \infty)$ which with an improper uniform prior spanning $(l_1 - s_2, \infty)$.
145 This introduces some bias into the estimated variance [22], but has reduced computational cost and
146 improved numerical stability relative to the latent variable approach.

147 Our model now consists of a loglikelihood that is significantly easier to evaluate, however there are
148 many latent variables present in the model. As a result, while it is now possible to fit the model in a
149 reasonable timeframe it cannot be considered fast. Many of these observations in the loglikelihood
150 will have identical values of s_1, s_2, l_1, l_2 . We now take advantage of this fact to develop an

151 approximate model that vastly reduces the number of latent variables, and consequently provides a
 152 significant improvement to the model fitting speed.

153 In our loglikelihood we have terms of the form

$$154 \quad L = \dots + \sum_{i \in G} \log(f_P(l_i^* - s_i^*)) + \sum_{i \in G} \log(f_L(l_i^*)) + \sum_{i \in G} \log(f_S(s_i^*)) + \dots$$

155 where G is a group of observations with identical values of s_1, s_2, l_1, l_2 .

156 As an approximation, we will introduce random variables \overline{S}_G and \overline{L}_G , representing the means of the
 157 latent variables s_i^* and l_i^* in group G . We will then approximate the loglikelihood as

$$158 \quad L \approx \dots + \sum_{i \in G} \log(f_P(\overline{L}_G - \overline{S}_G)) + \sum_{i \in G} \log(f_{\overline{L}_G}(\overline{L}_G)) + \sum_{i \in G} \log(f_{\overline{S}_G}(\overline{S}_G)) + \dots$$

$$159 \quad = \dots + n \log(f_P(\overline{L}_G - \overline{S}_G)) + n \log(f_{\overline{L}_G}(\overline{L}_G)) + n \log(f_{\overline{S}_G}(\overline{S}_G)) + \dots \quad (2)$$

160 where n is the number of observations in group G . Since the latent variables s_i^* and l_i^* have standard
 161 uniform prior distributions, the sample mean of our latent variables, \overline{L}_G and \overline{S}_G , are given by
 162 Bates(n) distributions. Since the computational complexity of the Bates likelihood function
 163 increases with n , to improve numerical efficiency we will approximate the Bates(n) distributions
 164 using Beta distributions. For the Bates(n), we have

$$165 \quad \mathbb{E}[\overline{S}_G] = \frac{1}{2}$$

$$166 \quad \text{Var}[\overline{S}_G] = \frac{1}{12n}.$$

167 To approximate this, we construct a Beta distribution with the same mean and variance. For the
 168 Beta distribution, we have

$$169 \quad \mathbb{E}[\overline{S}_G] = \frac{\alpha}{\alpha + \beta},$$

$$170 \quad \text{Var}[\overline{S}_G] = \frac{\alpha\beta}{(\alpha + \beta)^2(\alpha + \beta + 1)}.$$

171 Equating the means gives

$$172 \quad \frac{\alpha}{\alpha + \beta} = \frac{1}{2} \Rightarrow \alpha = \beta.$$

173 Equating the variances gives

$$174 \quad \frac{\alpha\beta}{(\alpha + \beta)^2(\alpha + \beta + 1)} = \frac{1}{12n} \Rightarrow \frac{(2\alpha)^2(2\alpha + 1)}{\alpha^2} = 12n \Rightarrow 8\alpha + 4 = 12n.$$

175 Therefore, we need $\alpha = \beta = \frac{3n-1}{2}$. An alternative approximation would be to use a normal
 176 distribution, which is accurate for large n due to the central limit theorem. For n between 1 and 12,
 177 we compare the Beta and Normal approximation in Supplementary Figure 1. In general, both
 178 approximations perform well, but the Beta distribution works better for small values of n , in
 179 particular $n = 1$ where it exactly yields the Uniform(0,1) distribution, as desired. Therefore, we opt
 180 to use the Beta approximation throughout. In our preliminary analysis, using the grouped
 181 approximation (Equation (2)) was found to lead to indistinguishable results with a substantial
 182 reduction in computational time.

183 Regardless of the censoring scenarios, the likelihood of the model depends on the distribution of the
184 positivity duration, either through the probability density function $f_p(\cdot)$ or cumulative distribution
185 function $F_p(\cdot)$. The duration of positivity is assumed to follow a right-skewed distribution with a non-
186 zero mode, since positivity cannot end instantaneously. Since viral load distributions vary with age
187 [25–27], we assume this distribution can vary with age group. To model this distribution, we assume
188 a lognormal distribution, parameterised by the log-mean, $\theta_{1,i}$, and log-standard-deviation, $\theta_{2,i}$,
189 parameters, which represent the mean and standard deviation of the logarithm of the distribution,
190 for age group i . The log-mean parameter is assumed to vary with age, following a hierarchical
191 structure, and we assume the log-standard-deviation parameter is fixed for all age groups, i.e. $\theta_{2,i} =$
192 θ_2 for all i . We model the parameters and latent variables using the following priors,

$$\begin{aligned} 193 \quad & \theta_{1,i} = \theta_1 + \beta_i \sigma_1, \\ 194 \quad & \theta_1 \sim N(0.5, 2.5^2), \\ 195 \quad & \theta_2 \sim \text{InverseGamma}(10, 2), \\ 196 \quad & \beta_i \sim N(0, 1), \\ 197 \quad & \sigma_1 \sim \text{Exp}(5), \\ 198 \quad & \bar{l}_G \sim \text{Beta}\left(\frac{3n_G - 1}{2}, \frac{3n_G - 1}{2}\right), \\ 199 \quad & \bar{s}_G \sim \text{Beta}\left(\frac{3n_G - 1}{2}, \frac{3n_G - 1}{2}\right). \end{aligned}$$

200

201 This hierarchical structure assumes that the log-mean parameter for each age group is centred
202 around an average value, with perturbations specific to each age group. These perturbations are
203 assumed to follow a normal distribution with mean of zero and variance of one. The sigma
204 parameter controls the magnitude of the perturbations, i.e. larger values of σ_1 allow individual age
205 groups to have larger deviations from the population average. Therefore, where an individual age
206 group has sparse data, the model will revert to the average value, and sufficient data is needed to
207 justify large deviations from the average value. These age effects are additive on the log-mean
208 parameter, which is roughly equivalent to a multiplicative effect on the linear scale (the effect is
209 multiplicative on the median of the modelled distribution). For example, the influence of age on the
210 median, relative to the population average, is a proportional change to the median duration of
211 positivity. For the latent variable priors (\bar{l}_G and \bar{s}_G), n_G is the number of observations in group G .

212 3.2. LFD test sensitivity

213 LFD tests are a powerful diagnostic tool due to a very short delay from testing to results. However,
214 this comes at a compromise of reduced sensitivity to small viral loads relative to the gold-standard
215 PCR tests. Therefore, when using LFD test results to monitor the epidemic, it is essential to quantify
216 the corresponding test sensitivity.

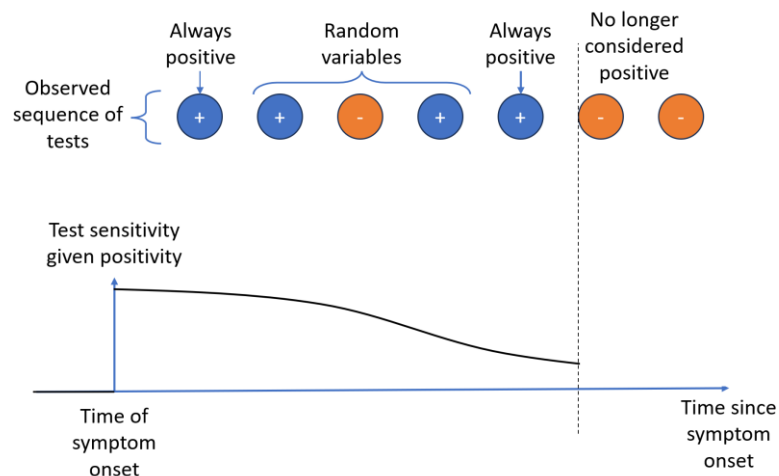
217 Test sensitivity is typically given/interpreted as the probability of obtaining a positive test result,
218 given that the tested individual is “currently infected”. There is, however, some ambiguity in how
219 “currently infected” is defined. In an ideal world, we might define “currently infected” to be
220 individuals who have not yet achieved viral clearance or who have a non-zero probability of
221 transmission, though in practice it is impossible to determine whether individuals are in either of
222 those states. Instead, surrogate definitions of “currently infected” are used. Most commonly, PCR

223 positivity is used as a surrogate for “currently infected”, where an individual is defined as “currently
224 infected” if there is a non-zero probability of returning a positive PCR result that is not a false
225 positive [14,28]. We note that this definition may not correspond to viral clearance, since PCR tests
226 can detect inactive viral fragments a significant length of time after the infection was cleared, nor
227 does it necessarily correspond to actively infectious cases for the same reason.

228 Since no PCR tests were used in this study, it is impossible to estimate the probability of obtaining a
229 positive LFD result given that an individual is PCR positive. Instead, our definition of “currently
230 infected” must be individuals who have a non-zero probability of returning a positive LFD test result
231 that is not a false positive. In other words, our definition of test positivity is the probability of
232 obtaining an LFD positive result, given that an individual’s infection could be detected by an LFD test.
233 As a result, if LFD sample positivity is adjusted to obtain the prevalence, the prevalence is defined as
234 “the prevalence of LFD positive individuals”. We consider sensitivity as a function of time since
235 symptom onset, as a proxy for time since infection. Therefore, this sensitivity tells us the probability
236 of correctly returning a positive test for someone who is still testing positive a specific number of
237 days after symptom onset. The period of the highest infectiousness is in the few days after symptom
238 onset [21], which also corresponds to the period of high LFD test sensitivity, suggesting our
239 definition of “currently infected” will capture the highly infectious individuals. We only consider
240 sensitivity after symptom onset, since we are treating this as the time of earliest positivity.

241 For inclusion in the test sensitivity model, we filter the repeat testing follow-up to individuals who
242 submitted an initial positive test in the main survey. For each individual, we observe a sequence of
243 test results starting with a positive, e.g. “positive, positive, negative, positive, negative, negative”
244 (Figure 1). The first test in this sequence will always be a positive result, as the individual would not
245 be included in the repeat testing data had they not tested positive in the main survey. Therefore, we
246 remove the first positive repeat testing result as it is not a random variable. It is assumed that once
247 an individual begins to return consecutive negative tests they are no longer in the positive state, i.e.
248 if the 6th and 7th tests are both negative, then the individual is no longer considered to be positive as
249 of the 6th test. Each testing sequence necessarily ends with a “positive, negative, negative”
250 subsequence, which implies the test prior to the first observation of two consecutive negatives must
251 be a positive test. Therefore, we also remove the last positive test as it is, by definition, a positive
252 test result and cannot be treated as a random variable. Since we are interested in sensitivity
253 conditional on still testing positive, all tests after the last positive test are also removed.

254



255

256

Figure 1: Schematic representation of the structure of the repeat testing data and model

257 This reduces the number of follow-up tests to 6758 tests. Individuals with unknown symptom onset
 258 date are removed, and individuals with negative time from symptom onset to test or symptom onset
 259 date 25 days or longer before testing date are also removed. This further reduces the number of
 260 positive tests to 6586, which forms our sample for the test sensitivity model. These tests were
 261 submitted by 3584 unique participants.

262 For each test included, we consider this data point as a pair of observations: the number of days
 263 from symptom onset, $d \in \mathbb{Z}_+$, drawn from a random variable D , and whether the test result, drawn
 264 from a random variable r , is positive ($r = 1$) or negative ($r = 0$). Since these data points are all
 265 conditional on the individual remaining in a positive state ($p = 1$), by aggregating the data by values
 266 of D , we can calculate the test sensitivity as a function of the time from symptom onset. Plotting the
 267 observed data (Supplementary Figure 2), we observe a sigmoidal shape to the data, with peak
 268 sensitivity at $D = 0$ and a plateau towards the end of the time period. This plateau occurs because
 269 we are conditional on individuals still testing positive, and restricting to a maximum of 24 days post
 270 symptom onset. If we increased the length of time since symptom onset, it is possible that a further
 271 decay in sensitivity would be observed. However, the probability of individuals still testing positive
 272 25 days or longer after symptom onset is very low, which would lead to very few data points to
 273 inform the model. To capture the observed sigmoidal behaviour, we use a generalised logistic
 274 function

$$275 \quad \mathbb{P}(r = 1|p = 1, D = d) = L + \frac{U - L}{1 + e^{-(s-gd)}}$$

276 where $L \in [0,1]$, $U \in [0,1]$, $s \in \mathbb{R}$, and $g \in \mathbb{R}_+$ are all parameters to be estimated. L and U
 277 represent the lower and upper bounds on the sensitivity, respectively. s is a parameter which shifts
 278 the curve, representing how soon sensitivity starts to decay. g is a rate parameter, which controls
 279 how quickly the sensitivity decays from the upper bound to the lower bound.

280 To fit the model, we aggregate the data such that for each value of D , we have the number of tests
 281 performed, $N_{\text{tests}}(d) \in \mathbb{Z}_+$, and the number of positive tests that occurred, $N_{\text{pos}}(d) \in \mathbb{Z}_{[0, N_{\text{tests}}(d)]}$, d
 282 days after symptom onset, in a population of cases that were still positive d days after symptom
 283 onset. We then assume that the observed number of positive tests is sampled from a binomial
 284 distribution with number of trials equal to total numbers of tests, and probability of success equal to
 285 $\mathbb{P}(r = 1|p = 1, D = d)$, i.e.

$$286 \quad N_{\text{pos}}(d) \sim \text{Binomial}(N_{\text{tests}}(d), \mathbb{P}(r = 1|p = 1, D = d)).$$

287 Test sensitivity will depend on the viral load of an individual at the time of their test. Since viral load
 288 trajectories will vary by age [25–27], test sensitivity is likely to vary with age [1]. To model this, we
 289 allow L and g to vary by age, and assume U and s are the same across all age groups, i.e.

$$290 \quad L_i \sim \text{Beta}(\mu_L \rho_L, (1 - \mu_L) \rho_L),$$

$$291 \quad \mu_L \sim \text{Beta}(4, 6),$$

$$292 \quad \rho_L \sim \text{Exp}(1).$$

$$293 \quad U \sim \text{Beta}(15, 1),$$

$$294 \quad g_i = \frac{1}{\mu_g + \beta_{g,i} \sigma_g},$$

$$\begin{aligned} 295 \quad & \beta_{g,i} \sim N(0,1), \\ 296 \quad & \sigma_g \sim \text{Exp}(1), \\ 297 \quad & \mu_g \sim N(1.5,1), \\ 298 \quad & s \sim N(4,3). \end{aligned}$$

299 A version of the model allowing all 4 parameters to vary by age was developed, but the U and s
300 parameters did not converge. The hierarchical structure for the rate parameter, g_i , acts on the
301 inverse as this aided convergence. This assumes that the inverse of the rate is affected by additive
302 perturbations due to the different age groups, where μ_g is the population average inverse rate
303 parameter and $\beta_{g,i}$ are age group specific perturbations with magnitude controlled by σ_g , which
304 leads to non-linear perturbations on the scale of the rate. The hierarchical structure for the lower
305 bound, L_i , assumes that the lower bound for each age group is sampled from a Beta distribution
306 with mean μ_L , and the ρ_L parameter controls the variance of this Beta distribution. This ensures all
307 lower bounds are bounded within the interval $(0,1)$, and allows different age groups to have
308 different lower bounds, but they are pulled towards the mean in the absence of data suggesting
309 otherwise.

310 3.3. Probability of testing positive over time

311 Instead of considering test sensitivity, which is conditional on the individual being in the infected
312 state, we may wish to calculate the probability that an individual returns a positive test result a
313 certain number of days after their infection began. This differs from the test sensitivity definition,
314 since this includes the probability that a negative test is returned because the individual has cleared
315 the infection. This also differs from the duration of positivity, since that tells us the probability of
316 whether an individual is still actively infected a certain number of days after infection began, rather
317 than the probability that a single test will return a positive result. The probability of returning a
318 positive a certain number of days after an infection is important, since it provides the relationship
319 between epidemic incidence and sample positivity which then informs modelling of the epidemic
320 trajectory.

321 As with the sensitivity and duration of positivity models, we will consider this as a function of time
322 since symptom onset, rather than time since infection. Therefore, this tells us the probability that a
323 test taken a certain number of days after the symptom onset date will return a true positive test
324 result, using LFD test positivity as a proxy for infection. Previous studies [13,29–33] have shown that
325 peak LFD sensitivity, which occurs around symptom onset, is comparable to peak PCR sensitivity,
326 which is considered the gold standard at detecting infection. Therefore, this will accurately describe
327 the probability of detecting an infection using LFD tests.

328 To calculate the probability of testing positive over time, we will use our results on test sensitivity
329 and duration of positivity. Letting $S(d)$ denote the probability of testing positive d days after
330 symptom onset, we have

$$331 \quad S(d) = \mathbb{P}(r = 1 | D = d) = \mathbb{P}(r = 1 \cap p = 1 | D = d),$$

332 since an individual can only return a true positive test ($r = 1$) if it is still possible for them to test
333 positive ($p = 1$). From this, we have

$$334 \quad S(d) = \mathbb{P}(r = 1 \cap p = 1 | D = d) = \frac{\mathbb{P}(r = 1 \cap p = 1 \cap D = d)}{\mathbb{P}(D = d)}$$

$$\begin{aligned} &= \frac{\mathbb{P}(r = 1 \cap p = 1 \cap D = d) \mathbb{P}(p = 1 \cap D = d)}{\mathbb{P}(p = 1 \cap D = d) \mathbb{P}(D = d)} \\ &= \mathbb{P}(r = 1 | p = 1 \cap D = d) \mathbb{P}(p = 1 | D = d) \\ &= \mathbb{P}(r = 1 | p = 1, D = d) (1 - F_p(d)), \end{aligned}$$

where $\mathbb{P}(r = 1 | p = 1, D = d)$ is the test sensitivity d days after symptom onset and $1 - F_p(d)$ is the complimentary cumulative distribution function of the duration of positivity.

3.4. Incubation period

The incubation period describes the time between an individual becoming infected and developing symptoms. Information on time of infection is challenging to obtain. Commonly, contact tracing data has been used, where the date of contact between a primary and secondary case can be used as a date of exposure [34], however contact tracing for SARS-CoV-2 is no longer performed in the UK. In the absence of contact tracing data other approaches must be taken. For example, at the beginning of the COVID-19 pandemic, time spent in Wuhan could be used to provide an approximate exposure window [35–37]. In this study, we investigate the potential of asking individuals to identify their exposure date. For some individuals this may be relatively easy, for example if they have contact with a highly symptomatic individual or have infrequent contacts. For individuals with frequent potential infectious contacts, the data quality is likely to be lower. To improve the reliability of the reported exposure dates, we limit this analysis to individuals in either 1 or 2 person households. This restriction is made since in larger households it can be challenging to identify the index case, leading to incorrectly identified exposure dates. The secondary event, symptom onset date, is easy to measure, and we ask individuals to report when they first developed symptoms.

For inclusion in the data for the incubation period model, we first select individuals with an estimated exposure date, which reduced the sample size to 3949. We then filtered the data to individuals in households of size 1 or 2, reducing the sample size to 2767. Individuals with symptom onset date on the 15th of any month were removed, since this was the default value if the question was not answered, reducing the sample size to 2089. Finally, individuals with inconsistent dates were removed, resulting in a final sample of 1405 individuals.

The incubation period describes the time between two epidemiological events, so we are interested in estimating the distribution of the possible time delays, since not all individuals will have the same value. In our data, the two events are time of exposure and time of symptom onset. Since not all infected individuals in the study will go on to develop symptoms, we only include an individual in our sample if they have developed symptoms. This introduces right truncation, whereby individuals with an exposure date within the study period but symptom onset date in the future were removed from our sample. This causes the observed time delay distribution to be biased towards shorter time delays. In this study, we are at the end of an epidemic wave, so the impact of the right-truncation will be minimal. In addition to the right truncation, our data are interval censored, since we only have an interval during which each event occurred, rather than the precise time. For both events, this interval censoring corresponded to a 24-hour window representing the day on which the event occurred. To correct for the interval censoring and right truncation, we use the Interval-censoring and right-truncation corrected approach (ICRTC) from [38]. Other potential approaches are described in [23], where this approach has been found to be the most accurate.

We consider two random variables, the time of exposure, E , and time of symptom onset, S , such that $E < S$. Our data takes the form of two intervals: the exposure window, $E \in [e_1, e_2]$; and the symptom onset window, $S \in [s_1, s_2]$, which each have a length of one day. The incubation period can be described by a random variable X which we assume follows a positive-valued right-skewed

379 distribution. We consider gamma, Weibull, and lognormal distributions, and assess goodness of fit
380 through Pareto Smoothed Importance Sampling Leave-One-Out (PSIS-LOO) cross validation [39]. For
381 each of these distributions, X is parameterised by two parameters, which we denote θ_1 and θ_2 . To
382 estimate these parameters, we consider the following interval-censoring and right-truncation
383 corrected likelihood function

$$384 \quad e^* \sim \text{Uniform}(e_1, e_2),$$

$$385 \quad s^* \sim \text{Uniform}(s_1, s_2),$$

$$386 \quad L = \frac{f_X(s^* - e^*)}{F_X(T - e^*)},$$

387 where f_X and F_X are the probability density function and cumulative distribution function,
388 respectively, of the incubation period.

389 In addition to the right-truncation and interval-censoring corrections, in the data there is a second
390 mode at zero, suggesting many respondents may have accidentally entered their symptom onset
391 date as their exposure date. Therefore, we remove such individuals from the study. To account for
392 this in the model, we additionally condition on the incubation period being larger than 1 day, which
393 changes the likelihood function to

$$394 \quad e^* \sim \text{Uniform}(e_1, e_2),$$

$$395 \quad s^* \sim \text{Uniform}(s_1, s_2),$$

$$396 \quad L = \frac{f_X(s^* - e^*)}{F_X(T - e^*) - F_X(1)}.$$

397 For each distribution, we parameterise the model such that θ_1 represents the log of the mean. θ_2
398 then represents the log of the standard deviation for the gamma and lognormal distributions, and
399 the log of the shape parameter for the Weibull distribution.

400 Incubation periods potentially vary by age since the severity of symptoms is highly sensitive to age.
401 To capture this, we consider a hierarchical version of the model, whereby θ_1 and θ_2 are age-specific
402 parameters. We model this as

$$403 \quad \log(\theta_{1,i}) = \log(\theta_1) + \beta_i \sigma_1,$$

$$404 \quad \log(\theta_{2,i}) = \log(\theta_2) + \alpha_i \sigma_2,$$

$$405 \quad \log(\theta_1) \sim \mathcal{N}(1, 2),$$

$$406 \quad \log(\theta_2) \sim \mathcal{N}(1.6, 1),$$

$$407 \quad \beta_i \sim \mathcal{N}(0, 1),$$

$$408 \quad \alpha_i \sim \mathcal{N}(0, 1),$$

$$409 \quad \sigma_1 \sim \text{Exp}(1),$$

$$410 \quad \sigma_2 \sim \text{Exp}(1).$$

411 This assumes a similar hierarchical structure to the other models. The hierarchical assumptions are
412 made on the logarithmic scale for the θ_1 (mean) and θ_2 parameters, which means that the influence
413 of age is multiplicative on the scale of the model parameters. For example, the influence of age on

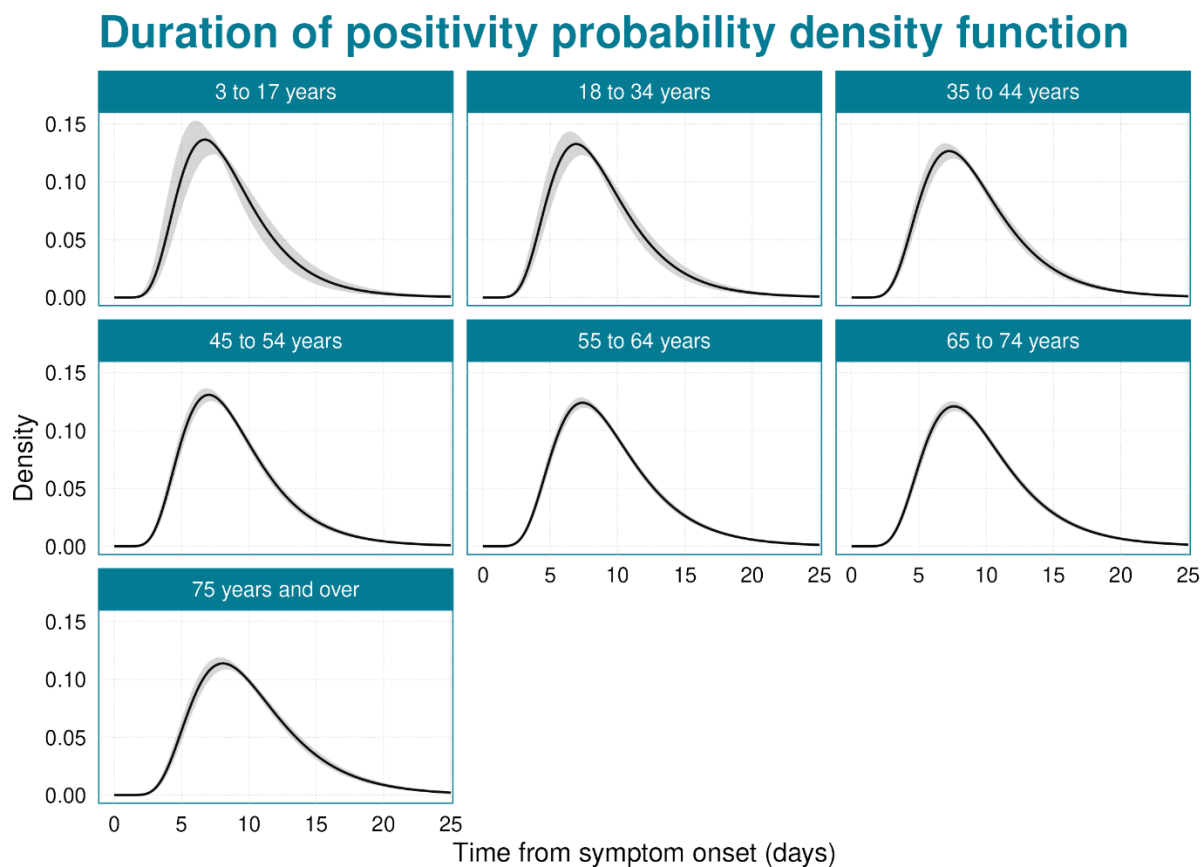
414 the mean, relative to the population average, is a proportional change to the mean incubation
415 period.

416 4. Results

417 4.1. Duration of positivity

418 For all age groups, the duration of positivity has very low early density (Figure 2) because very few
419 individuals are expected to stop testing positive in fewer than 2 days. This is consistent with the raw
420 data, where only 0.7% of doubly-interval censored data points had lower bounds on the duration of
421 positivity less than 2 days. Looking across age groups, there was significant variation in the duration
422 of positivity, though with high uncertainty in the youngest age groups (Figure 2, Table 2). The
423 youngest age group, 3 to 17 years, has the shortest mean duration of positivity, estimated at 8.55
424 days (95% Credible Interval (CrI): 7.65 days, 9.44 days), and as age increases there is an increasing
425 trend in the mean (with high uncertainty in some age groups), with the maximum mean duration of
426 positivity in the oldest age group, 75 years and over, with an estimate of 10.27 days (95% CrI: 9.85
427 days, 10.71 days). In addition to the mean increasing with age, the upper percentiles of the duration
428 of positivity also increases (Figure 3). For the 3 to 17 years age group, after 15.25 days (95% CrI:
429 13.63 days, 16.89 days), 95% of cases are no longer LFD positive. For the 75 years and over age
430 group, this increases to 18.31 days (95% CrI: 17.51 days, 19.19 days).

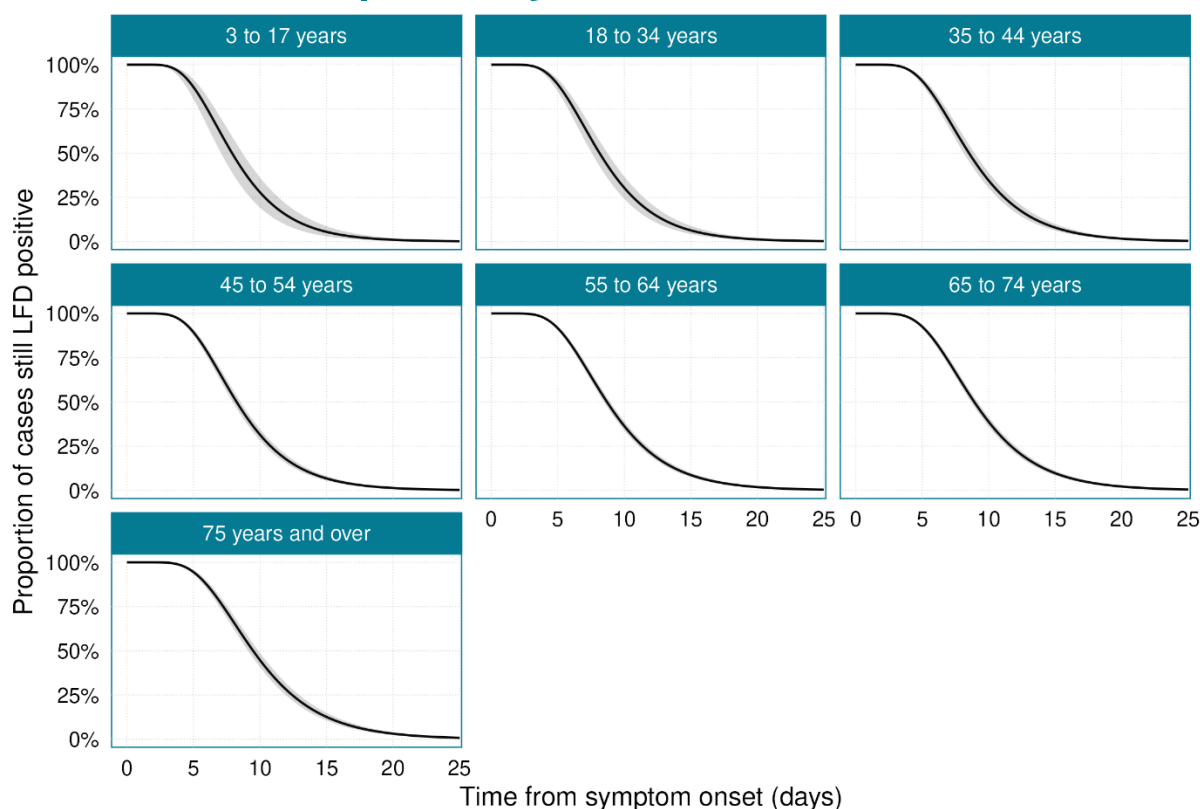
431 No data are shown for goodness of fit comparisons due to the censored nature of the data, with
432 each data point representing an interval of potential observations rather than a single observation,
433 so empirical PDFs/CDFs cannot be calculated.



434

435 **Figure 2:** Probability density function of the duration of positivity. The black line shows the median of the posterior
436 distribution, and the grey shaded region is the 95% credible interval.

Duration of positivity survival function



437

438 **Figure 3:** Probability that a case is still testing LFD positive. The black line shows the median of the posterior distribution,
 439 and the grey shaded region is the 95% credible interval.

440 **Table 2:** Mean, median, and 95th percentile of the duration of positivity distribution. The given estimates are medians of the
 441 posterior distribution, and the numbers in brackets are 95% credible intervals.

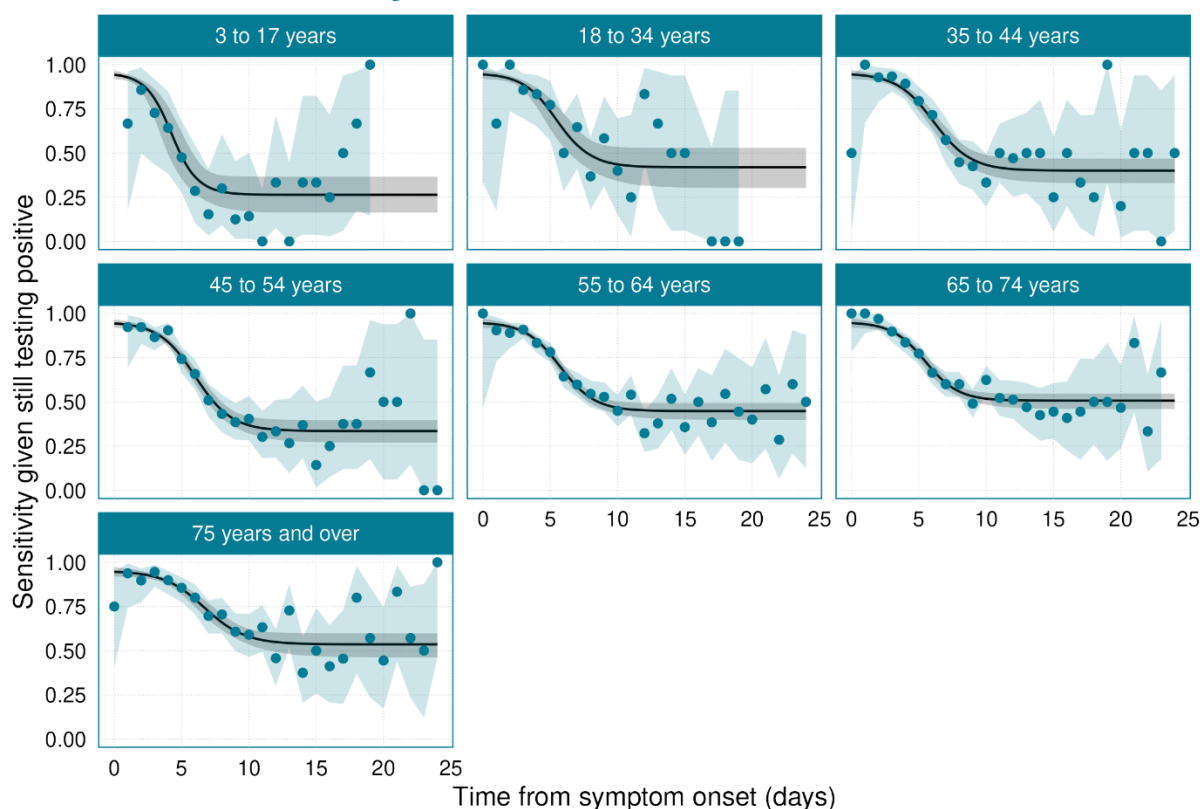
Age Group	Mean duration of positivity (days)	Median duration of positivity (days)	Duration of positivity 95 th percentile (days)
3 to 17 years	8.55 (95% CrI: 7.65, 9.44)	7.89 (95% CrI: 7.07, 8.71)	15.25 (95% CrI: 13.63, 16.89)
18 to 34 years	8.82 (95% CrI: 8.16, 9.45)	8.14 (95% CrI: 7.54, 8.73)	15.74 (95% CrI: 14.53, 16.92)
35 to 44 years	9.24 (95% CrI: 8.82, 9.68)	8.52 (95% CrI: 8.14, 8.93)	16.47 (95% CrI: 15.67, 17.32)
45 to 54 years	8.93 (95% CrI: 8.60, 9.25)	8.24 (95% CrI: 7.94, 8.53)	15.92 (95% CrI: 15.29, 16.58)
55 to 64 years	9.43 (95% CrI: 9.18, 9.69)	8.7 (95% CrI: 8.48, 8.94)	16.81 (95% CrI: 16.28, 17.40)
65 to 74 years	9.66 (95% CrI: 9.40, 9.94)	8.92 (95% CrI: 8.68, 9.17)	17.24 (95% CrI: 16.68, 17.83)
75 years and over	10.27 (95% CrI: 9.85, 10.71)	9.47 (95% CrI: 9.09, 9.88)	18.31 (95% CrI: 17.51, 19.19)

442

443 4.2. Sensitivity

444 Sensitivity is found to vary substantially with age (Figure 4, Table 3), with the minimum sensitivity
 445 increasing with increasing age. In the youngest age group, the minimum sensitivity is very low,
 446 plateauing at 0.26 (95% CrI: 0.16, 0.37). In the oldest age group, this increases to 0.54 (95% CrI: 0.46,
 447 0.60). Peak sensitivity was assumed to be equal across all age groups, with a peak of 0.95 (95% CrI:
 448 0.92, 0.98) at time of symptom onset. The rate at which sensitivity decays varied across age groups,
 449 with a pattern of decreasing decay rate with age. That is, not only does the youngest age group have
 450 the lowest lower bound, but it also reaches the minimum sensitivity the fastest.

Test sensitivity



451

452 **Figure 4:** Test sensitivity given a case is still testing positive. The black line shows the median of the posterior distribution,
 453 and the grey shaded region is the 95% credible interval. The blue points are the raw data, and the blue shaded region
 454 indicates beta distributed 95% confidence intervals around the raw data.

455 **Table 3:** Estimated parameters of the sensitivity model. The given estimates are medians of the posterior distribution, and
 456 the numbers in brackets are 95% credible intervals.

Age Group	Decay Rate	Lower bound	Upper bound	Shift
3 to 17 years	1.05 (95% CrI: 0.79, 1.44)	0.26 (95% CrI: 0.16, 0.37)	0.95 (95% CrI: 0.92, 0.98)	4.46 (95% CrI: 3.51, 5.66)
18 to 34 years	0.82 (95% CrI: 0.60, 1.12)	0.42 (95% CrI: 0.30, 0.53)	0.95 (95% CrI: 0.92, 0.98)	4.46 (95% CrI: 3.51, 5.66)
35 to 44 years	0.73 (95% CrI: 0.57, 0.94)	0.40 (95% CrI: 0.33, 0.47)	0.95 (95% CrI: 0.92, 0.98)	4.46 (95% CrI: 3.51, 5.66)
45 to 54 years	0.74 (95% CrI: 0.58, 0.96)	0.34 (95% CrI: 0.27, 0.40)	0.95 (95% CrI: 0.92, 0.98)	4.46 (95% CrI: 3.51, 5.66)
55 to 64 years	0.78 (95% CrI: 0.61, 1.00)	0.45 (95% CrI: 0.40, 0.49)	0.95 (95% CrI: 0.92, 0.98)	4.46 (95% CrI: 3.51, 5.66)
65 to 74 years	0.82 (95% CrI: 0.64, 1.04)	0.51 (95% CrI: 0.46, 0.55)	0.95 (95% CrI: 0.92, 0.98)	4.46 (95% CrI: 3.51, 5.66)
75 years and over	0.67 (95% CrI: 0.52, 0.87)	0.54 (95% CrI: 0.46, 0.60)	0.95 (95% CrI: 0.92, 0.98)	4.46 (95% CrI: 3.51, 5.66)

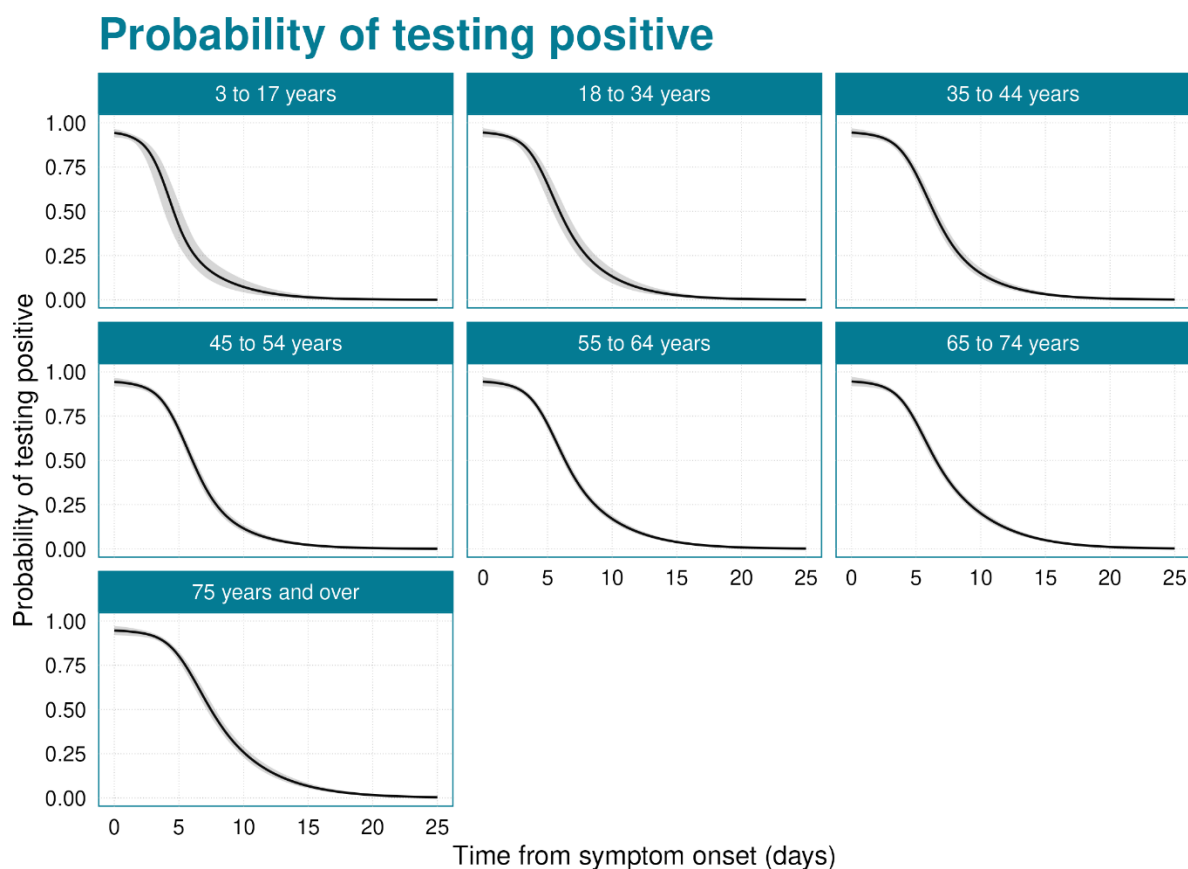
457

458 4.3. Probability of testing positive

459 In the probability of testing positive, we observe a large increasing effect of age (Figure 5), since this
 460 combines the age signals observed in both the test sensitivity and duration of positivity parameters.
 461 The probability of testing positive rapidly drops off, as time from symptom onset increases, in the
 462 youngest age groups, with a considerably slower decline for the oldest age group.

463 At zero days from symptom onset, all age groups had 95% (95% CrI: 92%, 98%) probability of testing
 464 positive (Table 4). For the youngest age group, by 4.8 days (95% CrI: 4.0 days, 5.4 days) from
 465 symptom onset, this drops to 50% probability of testing positive, dropping below 5% probability
 466 after 11.3 days (95% CrI: 9.7 days, 13.0 days). For the oldest age group, these thresholds are

467 increased to 7.6 days (95% CrI: 7.3 days, 8.0 days) and 16.2 days (95% CrI: 15.4 days, 17.1 days),
 468 respectively.



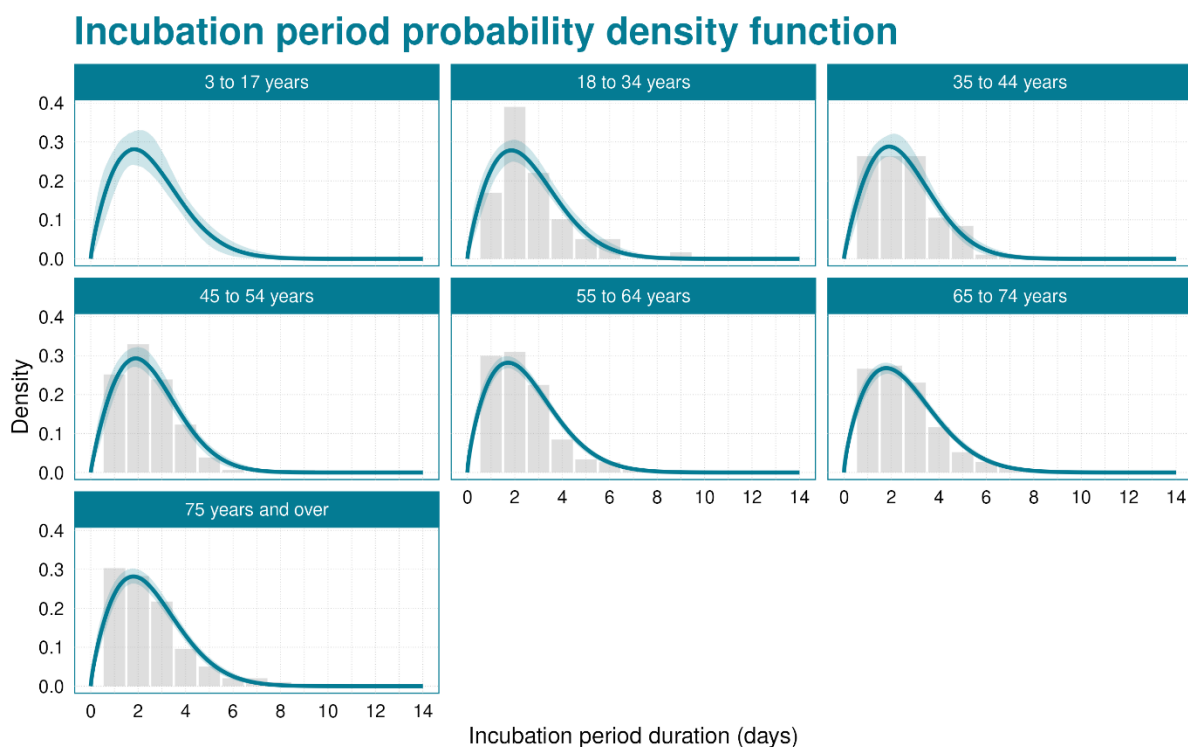
469
 470 **Figure 5:** Probability that an individual returns a positive LFD test result. The black line shows the median of the posterior
 471 distribution, and the grey shaded region is the 95% credible interval.

472 **Table 4:** Threshold values for time from symptom onset above which the probability of a test returning a negative result is
 473 above 50% and 95%. The given estimates are medians of the posterior distribution, and the numbers in brackets are 95%
 474 credible intervals.

Age Group	Threshold where 50% of tests are negative (days)	Threshold where 95% of tests are negative (days)
3 to 17 years	4.8 (95% CrI: 4.0, 5.4)	11.3 (95% CrI: 9.7, 13.0)
18 to 34 years	6.1 (95% CrI: 5.5, 6.6)	13.2 (95% CrI: 11.9, 14.4)
35 to 44 years	6.5 (95% CrI: 6.2, 6.8)	13.7 (95% CrI: 12.8, 14.5)
45 to 54 years	6.2 (95% CrI: 6.0, 6.4)	12.7 (95% CrI: 12.0, 13.4)
55 to 64 years	6.5 (95% CrI: 6.3, 6.7)	14.3 (95% CrI: 13.8, 14.9)
65 to 74 years	6.7 (95% CrI: 6.4, 6.9)	15.1 (95% CrI: 14.6, 15.7)
75 years and over	7.6 (95% CrI: 7.3, 8.0)	16.2 (95% CrI: 15.4, 17.1)

475
 476 **4.4. Incubation period**
 477 For the incubation period, there was no strong evidence of a difference between the model LOO
 478 scores estimated for each distribution (Supplementary Table 2). Weibull had the lowest estimated
 479 LOO, so all results are presented using a Weibull distribution, with gamma and lognormal
 480 distributions shown in Supplementary Table 3 and Supplementary Figures 3 and 4. There is no clear
 481 pattern in the incubation period with age (Figure 6, Table 5). Across all ages (Table 5), the mean
 482 incubation period was 2.52 days (95% CrI: 2.42 days, 2.62 days). The median incubation period was

483 slightly shorter, at 2.24 days (95% CrI: 2.14 days, 2.35 days). The 95th percentile of the incubation
 484 period, by which point we expect 95% of cases to have developed symptoms (Figure 7), was 5.53
 485 days (95% CrI: 5.31 days, 5.79 days).

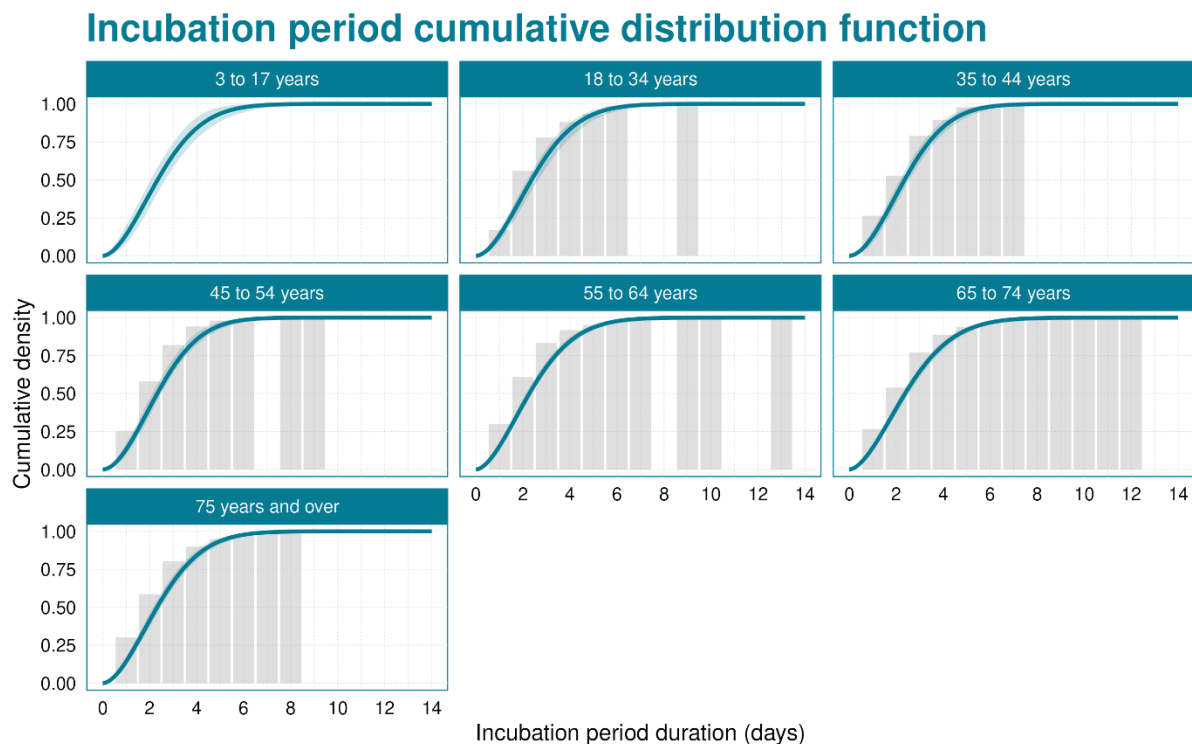


486
 487 **Figure 6:** Probability density function of the incubation period. The blue line shows the median of the posterior distribution,
 488 and the blue shaded region is the 95% credible interval. The grey histogram shows the raw data (the 3 to 17 years age
 489 group data are masked due to low counts).

490 **Table 5:** Mean, median and 95th percentile of the incubation period distribution. The given estimates are medians of the
 491 posterior distribution, and the numbers in brackets are 95% credible intervals.

Age Group	Mean Incubation Period	Median Incubation Period	95 th Percentile of the Incubation Period
All ages	2.52 (95% CrI: 2.42, 2.62)	2.24 (95% CrI: 2.14, 2.35)	5.53 (95% CrI: 5.31, 5.79)
3 to 17 years	2.55 (95% CrI: 2.25, 2.87)	2.34 (95% CrI: 2.04, 2.65)	5.25 (95% CrI: 4.44, 6.12)
18 to 34 years	2.57 (95% CrI: 2.39, 2.86)	2.37 (95% CrI: 2.18, 2.65)	5.31 (95% CrI: 4.83, 5.92)
35 to 44 years	2.54 (95% CrI: 2.35, 2.74)	2.35 (95% CrI: 2.16, 2.56)	5.12 (95% CrI: 4.65, 5.63)
45 to 54 years	2.50 (95% CrI: 2.31, 2.66)	2.32 (95% CrI: 2.11, 2.49)	5.03 (95% CrI: 4.60, 5.46)
55 to 64 years	2.50 (95% CrI: 2.36, 2.61)	2.27 (95% CrI: 2.13, 2.39)	5.26 (95% CrI: 4.96, 5.56)
65 to 74 years	2.62 (95% CrI: 2.50, 2.77)	2.38 (95% CrI: 2.25, 2.53)	5.54 (95% CrI: 5.25, 5.88)
75 years and over	2.53 (95% CrI: 2.36, 2.68)	2.31 (95% CrI: 2.14, 2.47)	5.25 (95% CrI: 4.89, 5.64)

492



493
494 **Figure 7:** Cumulative distribution function of the incubation period. The blue line shows the median of the posterior
495 distribution, and the blue shaded region is the 95% credible interval. The grey histogram shows the raw data (the 3 to 17
496 years age group data are masked due to low counts).

497 5. Discussion

498 The Winter Coronavirus Infection Survey in the UK has been a valuable source of information on the
499 SARS-CoV-2 virus. From this survey, data were collected that can support the estimation of
500 parameters that are of value to understanding the ongoing epidemiology of SARS-CoV-2. Given the
501 complexities of the data and real-world biases, statistical modelling methods are needed to
502 maximise the information extracted from the data. We have developed bespoke methods for
503 estimating the duration of positivity and test sensitivity, and deployed the gold standard method for
504 estimating the incubation period [23].

505 The duration of LFD positivity tells us how long after infection an individual remains able to test
506 positive using LFD tests. This is important, as if an individual takes a test too long after infection, it
507 may no longer be possible to test positive, and the infection will go undetected. Therefore,
508 quantifying this distribution is vital when using testing data for infectious disease surveillance. Also,
509 LFD positivity is closely linked to viral load in the individual [14]. The duration of positivity was
510 shortest for the youngest age groups and increased with age. This finding is consistent with data on
511 severity of infection, whereby older individuals are more likely to have severe disease [1,40,41].
512 Since severity is likely to correspond to higher viral load / slower viral clearance, this suggests that
513 the duration of positivity should be shorter in younger individuals, which has been seen in earlier
514 studies on the duration of viral shedding [25]. The duration of LFD positivity was found to have a
515 mean of 8.55 days (95% CrI: 7.65 days, 9.44 days) days for the youngest age group, which increased
516 with age to 10.27 days (95% CrI: 9.85 days, 10.71 days) in the oldest age group. Compared to
517 previous estimates for pre-Alpha variants [13], this has reduced slightly from a median of 11 days
518 (95% confidence interval: 10 days, 12 days) to a median of between 7.89 days (95% CrI: 7.07 days,
519 8.71 days) and 9.47 days (95% CrI: 9.09 days, 9.88 days), depending on the age of the individual.
520 Such a reduction in the duration of positivity could be due to the reduced severity of Omicron sub-
521 lineages [2–5] or higher levels of both infection-derived and vaccine-derived immunity. Based on the

522 fitted lognormal distributions, 95% of cases are no longer LFD positive between 13.63 days and
523 19.19 days after symptom onset, depending on age. In our duration of positivity data, we do not
524 have data on time of infection. Therefore, duration of positivity is considered as a function of time
525 from symptom onset. However, in practice some individuals can test positive prior to symptom
526 onset. In this study, such cases were very rare, suggesting that the probability of testing positive
527 prior to symptom onset was very low, so this assumption will have a minimal influence on the
528 results. The low probability of testing positive prior symptom onset is driven by antigen levels only
529 growing shortly before symptom onset [21].

530 Test sensitivity for LFD tests has previously been shown to be lower than the gold-standard PCR tests
531 [13,28,42]. However, despite the reduced sensitivity, due to the greatly improved time-to-result and
532 reduced cost, LFD tests can be a powerful tool in the response to the COVID-19 pandemic [43]. The
533 continued strength of LFDs relies on the test sensitivity remaining at similar levels, or increasing.
534 Early findings for Omicron suggested increased sensitivity (73.0%) relative to Alpha and Delta
535 variants (55.7% and 64.0%, respectively [14]). We estimated LFD test sensitivity as a function of time
536 from symptom onset. Here, the sensitivity is relative to individuals who are still able to test LFD
537 positive. It is possible that some individuals may never have high enough viral loads to test positive
538 by LFD. However, previous estimates suggest that peak LFD sensitivity is comparable to peak PCR
539 sensitivity [13]. LFD sensitivity at the peak was 95% (92%, 98%). This quickly decayed in all age
540 groups, though the minimum sensitivity varied by age. In the youngest age group, the minimum
541 sensitivity was lowest, at 0.26 (95% CrI: 0.16, 0.37). In the oldest age group, this increased to 0.54
542 (95% CrI: 0.46, 0.60). Not only did the youngest age groups have the lowest minimum sensitivity, but
543 they also had the fastest rate of decay from maximum to minimum sensitivity. Higher sensitivity in
544 older age groups supports the use of lateral flow tests in clinical settings [44], such as care homes,
545 where the majority of patients are elderly. In this analysis, we considered sensitivity as a function of
546 time since symptom onset. Often, sensitivity is reported as a single value [28,45]. From our temporal
547 sensitivity, comparable single values can be generated by weighting the sensitivity distribution by
548 the observed distribution of times from symptom onset for a given cohort. However, such figures
549 are not reported in this analysis since they are highly dependent on the cohort distribution, which
550 are not necessarily consistent between studies. Importantly, LFD test sensitivity in the few days
551 proceeding symptom onset is very high, which overlaps when individuals are most infectious [21]
552 and therefore enables efficient isolation of infectious individuals.

553 Based on the results for test sensitivity and duration of positivity, we calculated the probability of
554 testing positive as a function of time since symptom onset. Whereas sensitivity gives the probability
555 of testing positive given that someone is still infected, this instead gives the probability of testing
556 positive given the number of days ago that the individual was infected. This provides the relationship
557 between infection incidence and test positivity data, which is fundamental to accurate disease
558 surveillance. We found that the effect of age was further amplified, with the youngest age group
559 seeing rapid decline in the probability of testing positive, which slowed down as age increased. In
560 the youngest age group, after 4.8 days (95% CrI: 4.0 days, 5.4 days), 50% of tests would no longer
561 test positive, which increased to 7.6 days (95% CrI: 7.3 days, 8.0 days) in the oldest age group. After
562 11.3 days (95% CrI: 9.7 days, 13.0 days), fewer than 5% of tests in the youngest age group return a
563 positive test result. This 5% threshold increases to 16.2 days (95% CrI: 15.4 days, 17.1 days) in the
564 oldest age group. This shows that although LFD tests are reliable for detecting recent infection close
565 to time of infection (using symptom onset as a proxy), their sensitivity rapidly declines so that they
566 do not detect historic infections.

567 The incubation period describes the time between an individual becoming infected and eventually
568 developing symptoms. This is important in the design of isolation strategies, for example, where we
569 need to know how quickly people will develop symptoms after infection. At the start of the SARS-
570 CoV-2 pandemic, incubation period estimates ranged from 4.84 days to 6.4 days [35–37,46]. The
571 mean incubation period in this study was estimated at 2.52 days (95% CrI: 2.42 days, 2.62 days). This
572 is shorter than estimates of 2.6 days to 3.8 days for Omicron BA.5 [8,15], which is the most recent
573 variant with estimates in the literature. However, the incubation period was on a decreasing
574 trajectory since wild type [6,8], and with countless variants emerging since Omicron BA.4/5, it may
575 be possible for the incubation period to have decreased further. For example, influenza incubation
576 periods are even shorter at 1.71 days [47]. With this incubation period, 95% of individuals have
577 developed symptoms by 5.53 days (95% CrI: 5.31 days, 5.79 days). We found no patterns of changing
578 incubation periods with age, which is consistent with some previous studies [6], though others have
579 identified a weak relationship with age [48]. With the relatively small sample size, such a signal
580 would be hard to detect. The incubation period data relies on individuals estimating their time of
581 infection, which may introduce a bias. For some individuals, this may be accurate, such as those who
582 infrequently leave the house. For individuals in large households, these data are likely to be
583 inaccurate due to large number of potential infectors. To mitigate for this, we restricted the analysis
584 to 1 and 2 person households. However, in 2 person households, it is possible that pre-symptomatic
585 transmission can occur, which might bias the estimated exposure dates, leading to an underestimate
586 of the incubation period.

587 **6. Conclusion**

588 The Winter Coronavirus Infection Study, although designed to improve our understanding of SARS-
589 CoV-2 prevalence in the community, has been a valuable source of data on key epidemiological
590 parameters. The study design used will be powerful in future community surveillance studies for
591 allowing continued estimation of these parameters. Through this study, we have identified large
592 changes in the epidemiology. Firstly, the duration of LFD positivity for currently circulating variants
593 has reduced relative to pre-Omicron variants. Secondly, LFD test sensitivity remains high, particularly
594 shortly after symptom onset, when individuals are likely to be the most infectious. Finally, the
595 incubation period has been observed to have declined relative to earlier variants. Understanding the
596 current values of these parameters is essential for designing policy and interventions, as well as for
597 accurately converting test positivity data to estimates of infection incidence and prevalence, which
598 are vital for assessing real-time infection risk in the community.

599

600 **Ethics Approval**

601 The study received ethical approval from the National Statistician's Data Ethics Advisory Committee.

602

603 **Conflict of Interest**

604 The authors have declared that no competing interests exist. There was no financial support for this
605 work, completed as part of the authors' employment.

606

607 **Acknowledgements**

608 The authors would like to thank the UKHSA Surveillance and Immunity team and ONS WCIS analysis
609 team for their contributions.

610

611 **Data Availability Statement**

612 Stan code for all models and trace files from the MCMC samplers are available at
613 https://github.com/OvertonC/winter_covid_infection_study-parameters.

614
615 UKHSA operates a robust governance process for applying to access protected data that considers:
616

- 617 • the benefits and risks of how the data will be used
- 618 • compliance with policy, regulatory and ethical obligations
- 619 • data minimisation
- 620 • how the confidentiality, integrity, and availability will be maintained
- 621 • retention, archival, and disposal requirements
- 622 • best practice for protecting data, including the application of ‘privacy by design and by default’, emerging privacy conserving technologies and contractual controls

623 Access to protected data is always strictly controlled using legally binding data sharing contracts.
624 UKHSA welcomes data applications from organisations looking to use protected data for public
625 health purposes.
626 To request an application pack or discuss a request for UKHSA data you would like to submit, contact
627 DataAccess@ukhsa.gov.uk.
628

629 References

- 630 [1] Ward T, Fyles M, Glaser A, Paton RS, Ferguson W, Overton CE. The real-time infection
631 hospitalisation and fatality risk across the COVID-19 pandemic in England. *Nat Commun*
632 2024;15:4633. <https://doi.org/10.1038/s41467-024-47199-3>.
- 633 [2] Wolter N, Jassat W, Walaza S, Welch R, Moultrie H, Groome M, et al. Early assessment of the
634 clinical severity of the SARS-CoV-2 omicron variant in South Africa: a data linkage study. *Lancet*
635 *Lond Engl* 2022;399:437–46. [https://doi.org/10.1016/S0140-6736\(22\)00017-4](https://doi.org/10.1016/S0140-6736(22)00017-4).
- 636 [3] Ulloa AC, Buchan SA, Daneman N, Brown KA. Estimates of SARS-CoV-2 Omicron Variant
637 Severity in Ontario, Canada. *JAMA* 2022;327:1286–8. <https://doi.org/10.1001/jama.2022.2274>.
- 638 [4] Hyams C, Challen R, Marlow R, Nguyen J, Begier E, Southern J, et al. Severity of Omicron
639 (B.1.1.529) and Delta (B.1.617.2) SARS-CoV-2 infection among hospitalised adults: a
640 prospective cohort study in Bristol, United Kingdom. *Lancet Reg Health – Eur* 2023;25.
641 <https://doi.org/10.1016/j.lanepe.2022.100556>.
- 642 [5] Nyberg T, Ferguson NM, Nash SG, Webster HH, Flaxman S, Andrews N, et al. Comparative
643 analysis of the risks of hospitalisation and death associated with SARS-CoV-2 omicron
644 (B.1.1.529) and delta (B.1.617.2) variants in England: a cohort study. *The Lancet*
645 2022;399:1303–12. [https://doi.org/10.1016/S0140-6736\(22\)00462-7](https://doi.org/10.1016/S0140-6736(22)00462-7).
- 646 [6] Ward T, Glaser A, Overton CE, Carpenter B, Gent N, Seale AC. Replacement dynamics and the
647 pathogenesis of the Alpha, Delta and Omicron variants of SARS-CoV-2. *Epidemiol Infect*
648 2023;151:e32. <https://doi.org/10.1017/S0950268822001935>.
- 649 [7] UK Health Security Agency. COVID-19 Omicron variant: infectious period and asymptomatic
650 and symptomatic transmission. GOVUK 2024.
651 [https://www.gov.uk/government/publications/covid-19-omicron-variant-infectious-period-](https://www.gov.uk/government/publications/covid-19-omicron-variant-infectious-period-and-asymptomatic-and-symptomatic-transmission)
652 [and-asymptomatic-and-symptomatic-transmission](https://www.gov.uk/government/publications/covid-19-omicron-variant-infectious-period-and-asymptomatic-and-symptomatic-transmission) (accessed June 3, 2024).
- 653 [8] Xu X, Wu Y, Kummer AG, Zhao Y, Hu Z, Wang Y, et al. Assessing changes in incubation period,
654 serial interval, and generation time of SARS-CoV-2 variants of concern: a systematic review and
655 meta-analysis. *BMC Med* 2023;21:374. <https://doi.org/10.1186/s12916-023-03070-8>.
- 656 [9] Department of Health and Social Care. Liverpool COVID-19 community testing pilot: interim
657 evaluation report summary. GOVUK n.d.
658 [https://www.gov.uk/government/publications/liverpool-covid-19-community-testing-pilot-](https://www.gov.uk/government/publications/liverpool-covid-19-community-testing-pilot-interim-evaluation-report-summary/liverpool-covid-19-community-testing-pilot-interim-evaluation-report-summary)
659 [interim-evaluation-report-summary/liverpool-covid-19-community-testing-pilot-interim-](https://www.gov.uk/government/publications/liverpool-covid-19-community-testing-pilot-interim-evaluation-report-summary/liverpool-covid-19-community-testing-pilot-interim-evaluation-report-summary)
660 [evaluation-report-summary](https://www.gov.uk/government/publications/liverpool-covid-19-community-testing-pilot-interim-evaluation-report-summary/liverpool-covid-19-community-testing-pilot-interim-evaluation-report-summary) (accessed June 3, 2024).
- 661 [10] World Health Organization. Coronavirus disease (COVID-19): Contact tracing n.d.
662 [https://www.who.int/news-room/questions-and-answers/item/coronavirus-disease-covid-19-](https://www.who.int/news-room/questions-and-answers/item/coronavirus-disease-covid-19-contact-tracing)
663 [contact-tracing](https://www.who.int/news-room/questions-and-answers/item/coronavirus-disease-covid-19-contact-tracing) (accessed June 3, 2024).

- 664 [11] Killingley B, Mann AJ, Kalinova M, Boyers A, Goonawardane N, Zhou J, et al. Safety, tolerability
665 and viral kinetics during SARS-CoV-2 human challenge in young adults. *Nat Med* 2022;28:1031–
666 41. <https://doi.org/10.1038/s41591-022-01780-9>.
- 667 [12] UK Health Security Agency. Winter Coronavirus (COVID-19) Infection Study: quality and
668 methodology information. GOVUK n.d. [https://www.gov.uk/government/statistics/winter-](https://www.gov.uk/government/statistics/winter-coronavirus-covid-19-infection-study-estimates-of-epidemiological-characteristics-england-and-scotland-2023-to-2024/winter-coronavirus-covid-19-infection-study-quality-and-methodology-information)
669 [coronavirus-covid-19-infection-study-estimates-of-epidemiological-characteristics-england-](https://www.gov.uk/government/statistics/winter-coronavirus-covid-19-infection-study-estimates-of-epidemiological-characteristics-england-and-scotland-2023-to-2024/winter-coronavirus-covid-19-infection-study-quality-and-methodology-information)
670 [and-scotland-2023-to-2024/winter-coronavirus-covid-19-infection-study-quality-and-](https://www.gov.uk/government/statistics/winter-coronavirus-covid-19-infection-study-estimates-of-epidemiological-characteristics-england-and-scotland-2023-to-2024/winter-coronavirus-covid-19-infection-study-quality-and-methodology-information)
671 [methodology-information](https://www.gov.uk/government/statistics/winter-coronavirus-covid-19-infection-study-estimates-of-epidemiological-characteristics-england-and-scotland-2023-to-2024/winter-coronavirus-covid-19-infection-study-quality-and-methodology-information) (accessed June 3, 2024).
- 672 [13] Davis EL, Hollingsworth TD. Estimating LFT and qPCR test-sensitivity over time since infection
673 from a human challenge study 2022. <https://doi.org/10.1101/2022.10.18.22280274>.
- 674 [14] Eyre DW, Futschik M, Tunkel S, Wei J, Cole-Hamilton J, Saquib R, et al. Performance of antigen
675 lateral flow devices in the UK during the alpha, delta, and omicron waves of the SARS-CoV-2
676 pandemic: a diagnostic and observational study. *Lancet Infect Dis* 2023;23:922–32.
677 [https://doi.org/10.1016/S1473-3099\(23\)00129-9](https://doi.org/10.1016/S1473-3099(23)00129-9).
- 678 [15] Ogata T, Tanaka H. SARS-CoV-2 Incubation Period during the Omicron BA.5–Dominant Period
679 in Japan - Volume 29, Number 3—March 2023 - *Emerging Infectious Diseases journal* - CDC n.d.
680 <https://doi.org/10.3201/eid2903.221360>.
- 681 [16] Stan Development Team. Stan Modeling Language Users Guide and Reference Manual. 2024.
- 682 [17] Gabry J, Češnovar R, Johnson A. cmdstanr: R Interface to “CmdStan.” 2023.
- 683 [18] RStudio Team. RStudio: Integrated Development Environment for R. Boston, MA: RStudio,
684 PBC.; 2020.
- 685 [19] Vehtari A, Gelman A, Simpson D, Carpenter B, Bürkner P-C. Rank-Normalization, Folding, and
686 Localization: An Improved $R^{\hat{}}$ for Assessing Convergence of MCMC (with Discussion). *Bayesian*
687 *Anal* 2021;16:667–718. <https://doi.org/10.1214/20-BA1221>.
- 688 [20] Department of Health and Social Care. [Withdrawn] Self-isolation for those with COVID-19 can
689 end after 5 full days following 2 negative LFD tests. GOVUK 2022.
690 [https://www.gov.uk/government/news/self-isolation-for-those-with-covid-19-can-end-after-](https://www.gov.uk/government/news/self-isolation-for-those-with-covid-19-can-end-after-five-full-days-following-two-negative-lfd-tests)
691 [five-full-days-following-two-negative-lfd-tests](https://www.gov.uk/government/news/self-isolation-for-those-with-covid-19-can-end-after-five-full-days-following-two-negative-lfd-tests) (accessed July 1, 2024).
- 692 [21] UK Health Security Agency. PCR testing for SARS-CoV-2 during the COVID-19 pandemic. GOVUK
693 n.d. [https://www.gov.uk/government/publications/pcr-testing-for-sars-cov-2-during-the-](https://www.gov.uk/government/publications/pcr-testing-for-sars-cov-2-during-the-covid-19-pandemic)
694 [covid-19-pandemic](https://www.gov.uk/government/publications/pcr-testing-for-sars-cov-2-during-the-covid-19-pandemic) (accessed July 1, 2024).
- 695 [22] Reich NG, Lessler J, Cummings DAT, Brookmeyer R. Estimating incubation period distributions
696 with coarse data. *Stat Med* 2009;28:2769–84. <https://doi.org/10.1002/sim.3659>.
- 697 [23] Park SW, Akhmetzhanov AR, Charniga K, Cori A, Davies NG, Dushoff J, et al. Estimating
698 epidemiological delay distributions for infectious diseases 2024:2024.01.12.24301247.
699 <https://doi.org/10.1101/2024.01.12.24301247>.
- 700 [24] Ward T, Johnsen A. Understanding an evolving pandemic: An analysis of the clinical time delay
701 distributions of COVID-19 in the United Kingdom. *PLOS ONE* 2021;16:e0257978.
702 <https://doi.org/10.1371/journal.pone.0257978>.
- 703 [25] Zheng S, Fan J, Yu F, Feng B, Lou B, Zou Q, et al. Viral load dynamics and disease severity in
704 patients infected with SARS-CoV-2 in Zhejiang province, China, January-March 2020:
705 retrospective cohort study. *BMJ* 2020;369:m1443. <https://doi.org/10.1136/bmj.m1443>.
- 706 [26] Xiao AT, Tong YX, Gao C, Zhu L, Zhang YJ, Zhang S. Dynamic profile of RT-PCR findings from 301
707 COVID-19 patients in Wuhan, China: A descriptive study. *J Clin Virol* 2020;127:104346.
708 <https://doi.org/10.1016/j.jcv.2020.104346>.
- 709 [27] Yan D, Liu X-Y, Zhu Y, Huang L, Dan B, Zhang G, et al. Factors associated with prolonged viral
710 shedding and impact of lopinavir/ritonavir treatment in hospitalised non-critically ill patients
711 with SARS-CoV-2 infection. *Eur Respir J* 2020;56. [https://doi.org/10.1183/13993003.00799-](https://doi.org/10.1183/13993003.00799-2020)
712 [2020](https://doi.org/10.1183/13993003.00799-2020).

- 713 [28] Mistry DA, Wang JY, Moeser M-E, Starkey T, Lee LYW. A systematic review of the sensitivity
714 and specificity of lateral flow devices in the detection of SARS-CoV-2. *BMC Infect Dis*
715 2021;21:828. <https://doi.org/10.1186/s12879-021-06528-3>.
- 716 [29] Quantifying the relationship between SARS-CoV-2 viral load and infectiousness | eLife n.d.
717 <https://elifesciences.org/articles/69302> (accessed June 8, 2024).
- 718 [30] He X, Lau EHY, Wu P, Deng X, Wang J, Hao X, et al. Temporal dynamics in viral shedding and
719 transmissibility of COVID-19. *Nat Med* 2020;26:672–5. [https://doi.org/10.1038/s41591-020-](https://doi.org/10.1038/s41591-020-0869-5)
720 0869-5.
- 721 [31] Hakki S, Zhou J, Jonnerby J, Singanayagam A, Barnett JL, Madon KJ, et al. Onset and window of
722 SARS-CoV-2 infectiousness and temporal correlation with symptom onset: a prospective,
723 longitudinal, community cohort study. *Lancet Respir Med* 2022;10:1061–73.
724 [https://doi.org/10.1016/S2213-2600\(22\)00226-0](https://doi.org/10.1016/S2213-2600(22)00226-0).
- 725 [32] Jones TC, Biele G, Mühlemann B, Veith T, Schneider J, Beheim-Schwarzbach J, et al. Estimating
726 infectiousness throughout SARS-CoV-2 infection course. *Science* 2021;373:eabi5273.
727 <https://doi.org/10.1126/science.abi5273>.
- 728 [33] Stankiewicz Karita HC, Dong TQ, Johnston C, Neuzil KM, Paasche-Orlow MK, Kissinger PJ, et al.
729 Trajectory of Viral RNA Load Among Persons With Incident SARS-CoV-2 G614 Infection (Wuhan
730 Strain) in Association With COVID-19 Symptom Onset and Severity. *JAMA Netw Open*
731 2022;5:e2142796. <https://doi.org/10.1001/jamanetworkopen.2021.42796>.
- 732 [34] Manica M, Litvinova M, Bellis AD, Guzzetta G, Mancuso P, Vicentini M, et al. Estimation of the
733 incubation period and generation time of SARS-CoV-2 Alpha and Delta variants from contact
734 tracing data. *Epidemiol Infect* 2023;151:e5. <https://doi.org/10.1017/S0950268822001947>.
- 735 [35] Backer JA, Klinkenberg D, Wallinga J. Incubation period of 2019 novel coronavirus (2019-nCoV)
736 infections among travellers from Wuhan, China, 20–28 January 2020. *Eurosurveillance*
737 2020;25:2000062. <https://doi.org/10.2807/1560-7917.ES.2020.25.5.2000062>.
- 738 [36] Overton CE, Stage HB, Ahmad S, Curran-Sebastian J, Dark P, Das R, et al. Using statistics and
739 mathematical modelling to understand infectious disease outbreaks: COVID-19 as an example.
740 *Infect Dis Model* 2020;5:409–41. <https://doi.org/10.1016/j.idm.2020.06.008>.
- 741 [37] Linton NM, Kobayashi T, Yang Y, Hayashi K, Akhmetzhanov AR, Jung S, et al. Incubation Period
742 and Other Epidemiological Characteristics of 2019 Novel Coronavirus Infections with Right
743 Truncation: A Statistical Analysis of Publicly Available Case Data. *J Clin Med* 2020;9:538.
744 <https://doi.org/10.3390/jcm9020538>.
- 745 [38] Ward T, Christie R, Paton RS, Cumming F, Overton CE. Transmission dynamics of monkeypox in
746 the United Kingdom: contact tracing study. *BMJ* 2022;379:e073153.
747 <https://doi.org/10.1136/bmj-2022-073153>.
- 748 [39] Vehtari A, Gelman A, Gabry J. Practical Bayesian model evaluation using leave-one-out cross-
749 validation and WAIC. *Stat Comput* 2017;27:1413–32. [https://doi.org/10.1007/s11222-016-](https://doi.org/10.1007/s11222-016-9696-4)
750 9696-4.
- 751 [40] Verity R, Okell LC, Dorigatti I, Winskill P, Whittaker C, Imai N, et al. Estimates of the severity of
752 coronavirus disease 2019: a model-based analysis. *Lancet Infect Dis* 2020;20:669–77.
753 [https://doi.org/10.1016/S1473-3099\(20\)30243-7](https://doi.org/10.1016/S1473-3099(20)30243-7).
- 754 [41] Bonanad C, García-Blas S, Tarazona-Santabalbina F, Sanchis J, Bertomeu-González V, Fácila L, et al.
755 The Effect of Age on Mortality in Patients With COVID-19: A Meta-Analysis With 611,583
756 Subjects. *J Am Med Dir Assoc* 2020;21:915–8. <https://doi.org/10.1016/j.jamda.2020.05.045>.
- 757 [42] Pickering S, Batra R, Merrick B, Snell LB, Nebbia G, Douthwaite S, et al. Comparative
758 performance of SARS-CoV-2 lateral flow antigen tests and association with detection of
759 infectious virus in clinical specimens: a single-centre laboratory evaluation study. *Lancet*
760 *Microbe* 2021;2:e461–71. [https://doi.org/10.1016/S2666-5247\(21\)00143-9](https://doi.org/10.1016/S2666-5247(21)00143-9).
- 761 [43] Department of Health and Social Care. Performance of lateral flow devices during the COVID-
762 19 pandemic. GOVUK n.d. <https://www.gov.uk/government/publications/lateral-flow-device->

- 763 performance-data/performance-of-lateral-flow-devices-during-the-covid-19-pandemic
764 (accessed July 1, 2024).
- 765 [44] Department of Health and Social Care. Infection prevention and control (IPC) in adult social
766 care: acute respiratory infection (ARI). GOVUK n.d.
767 [https://www.gov.uk/government/publications/infection-prevention-and-control-in-adult-](https://www.gov.uk/government/publications/infection-prevention-and-control-in-adult-social-care-acute-respiratory-infection/infection-prevention-and-control-ipc-in-adult-social-care-acute-respiratory-infection-ari)
768 [social-care-acute-respiratory-infection/infection-prevention-and-control-ipc-in-adult-social-](https://www.gov.uk/government/publications/infection-prevention-and-control-ipc-in-adult-social-care-acute-respiratory-infection/infection-prevention-and-control-ipc-in-adult-social-care-acute-respiratory-infection-ari)
769 [care-acute-respiratory-infection-ari](https://www.gov.uk/government/publications/infection-prevention-and-control-ipc-in-adult-social-care-acute-respiratory-infection/infection-prevention-and-control-ipc-in-adult-social-care-acute-respiratory-infection-ari) (accessed June 3, 2024).
- 770 [45] Böger B, Fachi MM, Vilhena RO, Cobre AF, Tonin FS, Pontarolo R. Systematic review with meta-
771 analysis of the accuracy of diagnostic tests for COVID-19. *Am J Infect Control* 2021;49:21–9.
772 <https://doi.org/10.1016/j.ajic.2020.07.011>.
- 773 [46] Lauer SA, Grantz KH, Bi Q, Jones FK, Zheng Q, Meredith HR, et al. The Incubation Period of
774 Coronavirus Disease 2019 (COVID-19) From Publicly Reported Confirmed Cases: Estimation and
775 Application. *Ann Intern Med* 2020;172:577–82. <https://doi.org/10.7326/M20-0504>.
- 776 [47] Boëlle P-Y, Ansart S, Cori A, Valleron A-J. Transmission parameters of the A/H1N1 (2009)
777 influenza virus pandemic: a review. *Influenza Other Respir Viruses* 2011;5:306–16.
778 <https://doi.org/10.1111/j.1750-2659.2011.00234.x>.
- 779 [48] Galmiche S, Cortier T, Charmet T, Schaeffer L, Chény O, Platen C von, et al. SARS-CoV-2
780 incubation period across variants of concern, individual factors, and circumstances of infection
781 in France: a case series analysis from the ComCor study. *Lancet Microbe* 2023;4:e409–17.
782 [https://doi.org/10.1016/S2666-5247\(23\)00005-8](https://doi.org/10.1016/S2666-5247(23)00005-8).
- 783